Original Research

Experimental Determination of Attenuation Coefficients in Tissue Equivalents

Lina Asker Muhammad Ali [1], Rasha Hamid Ahmed [1], Mohsin Hassan Ali [1*]

[1] Department of Physics, College of Education for Pure Sciences, Tikrit University, Tikrit 34001, Iraq
* Correspondence: muhsin.astro@tu.edu.iq

Received: November 12, 2025; Accepted: March 13, 2026

Abstract: In this work, the gamma-ray attenuation characteristics of epoxy resin composites reinforced with potassium chloride (KCl) were experimentally investigated. Different weight fractions of potassium chloride particles were tested to see how they affected the way gamma rays were absorbed. The acquired gamma ray spectra resulted from channels of americium, cesium and radium through a thallium-doped sodium iodide spectrometer (NaI(Th)). The detector was placed 15 cm from the source and collected for 900 s that were long enough to distinguish the light peak count, which corresponds to the emitted gamma photon.The optimal results among equivalent tissues corresponded to the 10% reinforcement ratio samples in measurements intended to obtain linear and mass attenuation coefficients. Large discrepancies were observed, but the relative differences between those outcomes and ICRU-44 values did not exceed 7% and demonstrated high potentials of these materials as a replacement for conventional radiation protective and biological ones.

Keywords: attenuation coefficients, gamma radiation, equivalent tissues, potassium chloride (KCl)

1. Introduction

Tissue-equivalent materials play a critical role in medical physics, particularly in applications related to radiation dosimetry, diagnostic imaging, nuclear medicine, and radiotherapy quality assurance. These materials are designed to reproduce the radiation interaction characteristics of human tissues, enabling accurate dose measurements, calibration of imaging systems, and verification of treatment planning and radiation protection procedures. The increasing clinical use of ionizing radiation has therefore intensified the demand for reliable and cost-effective tissue-equivalent materials that closely match reference tissue data over medically relevant photon energy ranges [1,2].

Polymer-based composites have gained considerable attention as tissue-equivalent candidates due to their mechanical stability, ease of fabrication, chemical durability, and low production cost. Among polymer matrices, epoxy resins are particularly attractive because their attenuation properties can be systematically tailored through the incorporation of suitable inorganic fillers. By adjusting filler concentration, key parameters such as density, effective atomic number, and electron density can be controlled, enabling epoxy-based composites to closely simulate the attenuation behavior of human soft tissues [3,4].

Although potassium chloride (KCl) is a well-known compound, its importance in tissue-equivalent materials lies in its ability to modify the effective atomic number and photon

interaction probability of polymer matrices. When incorporated into epoxy resin, KCl allows controlled tuning of gamma-ray attenuation properties, leading to improved agreement with soft-tissue reference data. Consequently, epoxy–KCl composites are promising candidates for phantom construction, dosimetric calibration blocks, and radiation shielding assessment in medical environments, where accurate simulation of tissue response to ionizing radiation is required [5,6].

In recent years, numerous studies have focused on the development and optimization of tissue-equivalent materials for medical radiation applications, emphasizing the importance of matching experimentally measured attenuation coefficients with standard reference data. Recent investigations have demonstrated that optimizing composite composition and considering photon energy dependence can significantly enhance tissue equivalence and dosimetric accuracy [7–11]. These studies highlight the growing interest in polymer-based composites as effective alternatives to conventional tissue substitutes such as polyethylene and paraffin.

The primary objective of the present study is to experimentally determine the linear attenuation coefficient, mass attenuation coefficient, and mean free path of epoxy resin composites loaded with different weight fractions of potassium chloride. The selected photon energy range (60–662 keV) corresponds to energies commonly employed in diagnostic imaging, nuclear medicine, and radiotherapy quality assurance, rather than therapeutic dose delivery. By comparing the experimentally obtained attenuation parameters with reference values reported in the ICRU-44 report [12], this work aims to evaluate the suitability of epoxy–KCl composites as reliable and cost-effective tissue-equivalent materials for medical radiation applications.

2. Theoretical part

The linear attenuation coefficient is an important quantity that describes how much of a beam's photons are absorbed or scattered over some length scale and is denoted by the units in cm^{-1}. It is defined based on Beer-Lambert equation [16] as:

$$I(x) = I_0 e^{-\mu_\ell X} \tag{1}$$

Where I is the intensity of the transmitted beam, I_0 denotes incident beam intensity and X stands for absorbing material thickness.

This characteristic parameter is crucial in evaluating the penetration capability of gamma-photons through shielding materials; it integrates both photon energy and atomic or effective atomic number Z eff for the target. On the other hand, mass attenuation coefficient (μ_m) indicates how frequently photons interact per unit mass at each area unit (cm^2/g), and can be described as follows [16]:

$$\mu_m = \frac{\mu_l}{\rho} = \frac{Ln\frac{I_0}{I}}{\rho x} \tag{2}$$

where ρ is the density of that material.

The uncertainty in the experimental results obtained in this study arises from the mass attenuation coefficient. The maximum error in the calculated mass attenuation coefficients was determined using error propagation, taking into account uncertainties in the incident intensity (I_0),

transmitted intensity (I), and the sample's areal density (t). The propagation of error formula is given by the following [17]:

$$\Delta\mu_m = \frac{1}{\rho x}\sqrt{\left(\frac{\Delta I_0}{I}\right)^2 + \left(\frac{\Delta I}{I}\right)^2 + \left(ln\frac{I_0}{I}\right)^2 + \left(\frac{\Delta\rho}{\rho}\right)^2 + \left(\frac{\Delta x}{x}\right)^2} \qquad (3)$$

These interactions are strongly dependent on the photon energy and the electron density. It should be mentioned that μ_m decrease quickly with the increasing of photon energy. In addition, we consider m.f.p. as the typical distance traveled by a single particle in the sample before to find two consecutive interactions with this material. It is calculated as follows [16]:

$$\lambda(cm) = \frac{\int_0^\infty x.e^{\mu_l x}dx}{\int_0^\infty e^{\mu_l x}dx} = \frac{1}{\mu_l} \qquad (4)$$

where λ is mean free path in cm, μ_l is again linear attenuation coefficient in cm^{-1}. While these principles form a theoretical foundation for radiation physics they also emphasize how the various phenomena and technologies related to gamma rays, such as those encountered in medical imaging and radiation protection, are actually applicable, making this required information for anyone working with gamma-ray technology today.

3. Experimental Part

3.1. Preparation of samples

The samples were produced by the open-mold method, which is regarded as an easy and effective method for the formation of plastic material. Several round plastic models (volume 13.2 cm^3, diameter 2.9 cm and height 0.5 cm) were tested. The molds were thoroughly cleaned before I used them and paraffin wax was spread over the inside to aid in removal of the samples and make it more difficult for samples to adhere. In order to obtain samples that did not require support, and as an example of a question, Sikadur-52 LP epoxy resin (1.06 g/cm^3) The epoxy resin is mainly composed of carbon, hydrogen, and oxygen, which are the dominant elements commonly reported for epoxy-based polymers. Based on the average elemental composition, the epoxy matrix can be represented by an approximate chemical formula of $C_{48}H_{96}O_6$, which corresponds to a scaled representation of the empirical formula. The atomic weights of the constituent elements are 12.01 g/mol for carbon (C), 1.008 g/mol for hydrogen (H), and 16.00 g/mol for oxygen (O). was slowly mixed at 250 r.p.m. using a handheld mix made in China. The hardener was mixed with the epoxy according to instructions for a volume ratio of 1:2, as required by the mold. When the paste was made it was placed into the molds and allowed to set at room temperature until firm. This step took 24 hours for most of the samples. After the samples were fully cured, they were removed from the molds and considered ready for additional processing. In addition, the epoxy glue with potassium chloride (KCl) was prepared by mixing 1.98 g/cm^3 of KCl from EDU TEK, INDIA. The weights of this addition were; 0%, 2%, 4%, 6%, 8%,10%,12% and 14%. A 0.01 mg precision balance with special attachment made in Japan was used to weigh the base material (epoxy glue) and reinforcing filler (potassium chloride). The following equation [16] was applied to determine the weight of the sample:

$$m_s = V_s x \rho_{sample} \qquad (5)$$

Where ρ_{sample} represents the density of the composite sample (g/cm³), m_s denotes the measured mass of the sample (g), and V_s refers to the sample volume (cm³), which was determined from the known dimensions of the mold.

The densities of the samples were determined using Archimedes' principle, as expressed by the following equation[17].

$$\rho_s = W_a/(W_a - W_w)\rho_w \quad (6)$$

Where W_a and W_w denote the weights of the sample in air and water, respectively, and ρ_w represents density of water.

Eight prepared samples were produced (A-H), which were engineered to mimic human tissue and contained different quantities of potassium chloride (KCl) and epoxy. The percentages of potassium chloride present in each sample are shown in Table 1, with materials formed from epoxy resin and potassium chloride samples A to H in Fig. 1, which show specimens that replicate human tissue.

Table 1. Percentage of potassium chloride (KCl) in each sample.

sample	Percentage of Epoxy resin (%)	Percentage of Potassium chloride (KCl) (%)	Mass of composites in air(g)	Mass of composites in water(g)	Density of composites (g/cm³)
A	100	0	14.000	0.7920	1.060±0.0161
B	98	2	14.234	1.0296	1.078±0.0164
C	96	4	14.477	1.2672	1.096±0.0166
D	94	6	14.720	1.518	1.115±0.0169
E	92	8	14.963	1.7556	1.133±0.0172
F	90	10	15.206	2.0064	1.152±0.0175
G	88	12	15.449	2.2440	1.170±0.0177
H	86	14	15.692	2.4816	1.188±0.0180

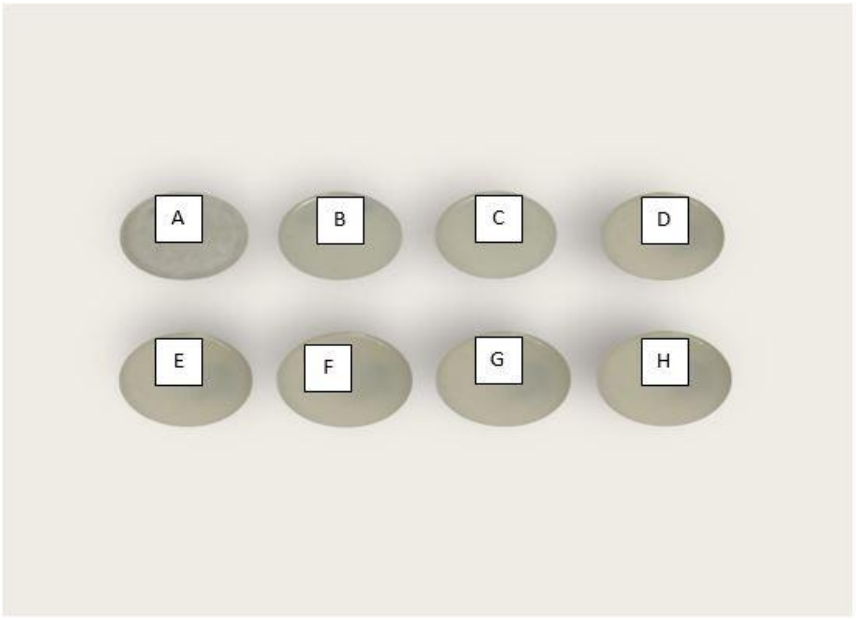

Fig 1. Human tissue equivalent specimens created utilizing epoxy resin materials combined with potassium chloride (KCl) labeled A-H.

3.2. Experimental set up

The gamma ray emitters ^{241}Am, ^{137}Cs and ^{226}Ra were used with a gamma ray measurement system Integrated Computer Spectrometer (I.C.S.). The Integrated Computer Spectrometer (I.C.S.) system was manufactured by EDU-TEK Company, India. This computer process is executed by an external program with scintillation detector arranged as in Fig2. The main amplifier and preamplifier (AP-4) are under NaI(Tl) alumina positive potential. The NaI(Tl) scintillation detector exhibits an energy resolution of approximately 7–8% at 662 keV (^{137}Cs) The detector exhibits a typical energy-dependent response suitable for gamma-ray spectroscopy within the investigated photon energy range. A multi-channel analyzer enters the computer to obtain collection conditions, data of measurements and to evaluate the summary. Energy calibration (channel-to-energy conversion) was performed prior to measurements using standard gamma-ray sources (^{241}Am and ^{137}Cs). X-rays from the radioactive source passed through a rectangular lead spectroscope (20 × 10 × 5 cm) to produce converged beam of X-rays, aperture diameter 15 mm. Beer–Lambert attenuation coefficients for human tissues equivalent at 59.4–662 keV were calculated. These energy scales were chosen for radiation therapy, nuclear medicine and medical imaging purposes. The gamma-ray spectra were subsequently measured with a NaI(Tl) detector. A layer of lead safety cover was attached to the detector surface for shielding from radiation source. The attenuation evaluation can be performed with the NaI(Tl) detector, and samples were placed between this detector and radiation source using the NaI(Tl) to perform measurements. The intrinsic efficiency of the NaI(Tl) detector was not explicitly determined, since attenuation coefficients were obtained from relative transmission measurements performed under identical experimental geometry and counting conditions, leading to cancellation of detector efficiency effects. The accumulation time was set to 900 s. Peak image features such as maximum position, clear area and full width at half maximum (FWHM) were monitored using the Fare "U.S.X. P.C.I." software. The FWHM values were also used as an indicator of detector energy resolution and spectral quality. Attenuation coefficients of

the samples were then determined using gamma rays energy of radioactive sources (59.4 keV ^{241}Am, 662 keV and 186–609 keV ^{137}Cs and ^{226}Ra), respectively.

Fig 2. The illustration the experimental setup utilized for measuring the gamma ray spectrum.

Figures 3 and 4 show the spectral information measured with the U.S.X. P.C.I. program, featuring gamma-ray sources: ^{241}Am at 59.4 keV, ^{137}Cs at 662 keV, and from a series of energies what refers to as ^{226}Ra, which varies between from187 and 609 keV. These measurements were applied to estimate the attenuation coefficients for each sample, and background radiation both in presence of a samples and without them.

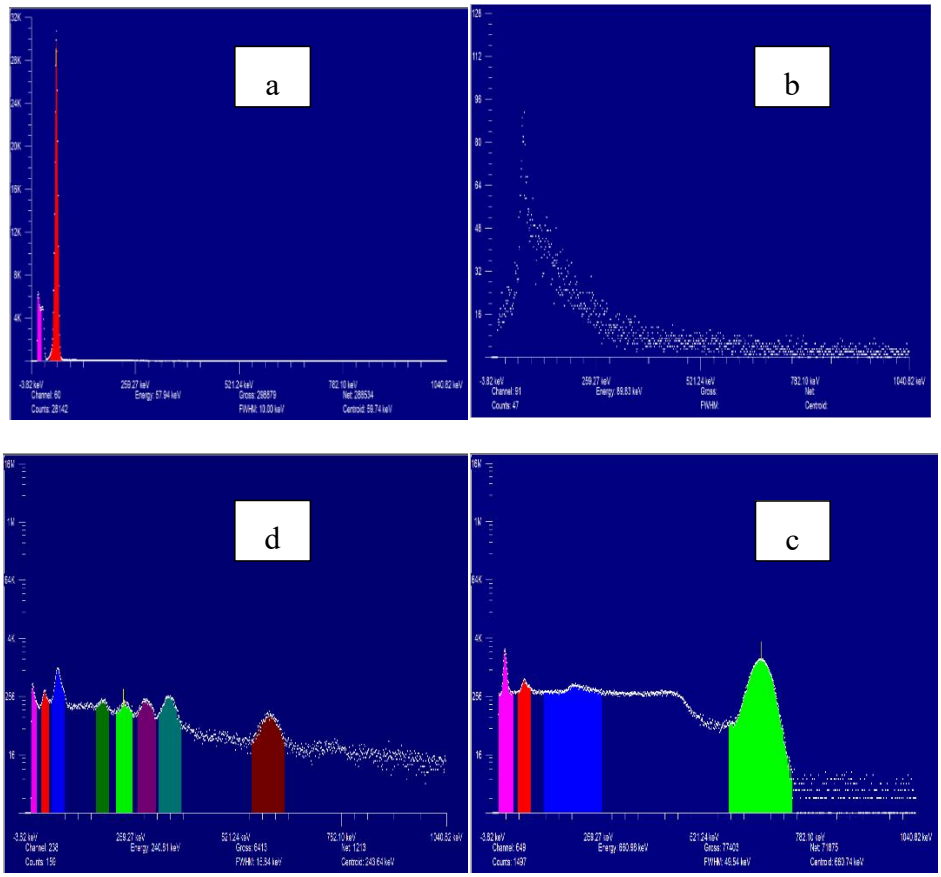

Fig 3. The gamma-ray spectroscopy results presented are categorized as follows: (a) background spectra, (b) ^{241}Am, (c) ^{137}Cs, and (d) ^{226}Ra.

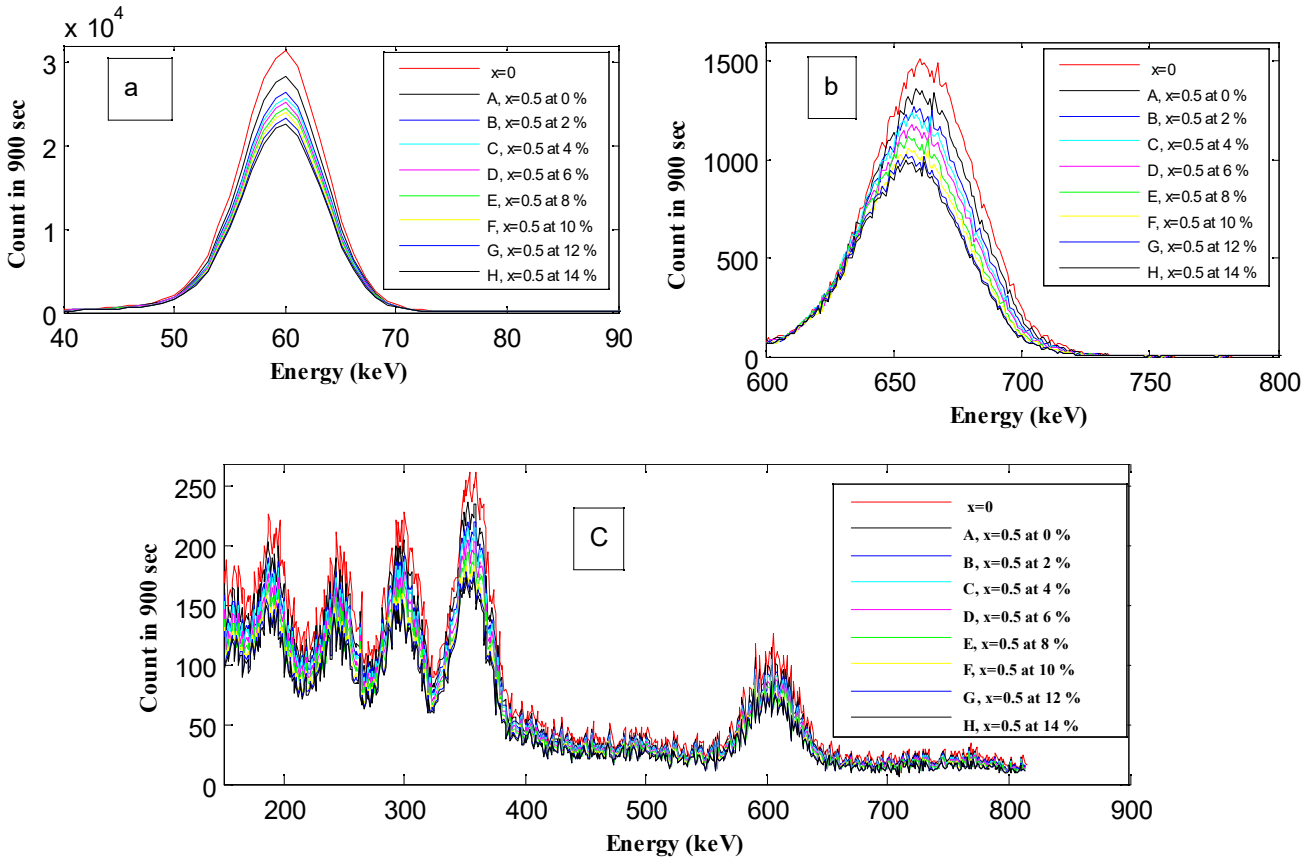

Fig 4. The spectrum acquired through γ-ray spectroscopy utilizing samples of (a) ^{241}Am, (b) ^{137}Cs, and (c) ^{226}Ra.

4. Results and discussion

4.1. Linear attenuation coefficients of potassium chloride (KCl) and epoxy

The linear attenuation coefficient (μ_l) of all prepared samples was determined using Eq. (1). The results of this test are found in Table 2. Finally, Figure 5 illustrates the relationship between the linear absorption coefficient and KCl to epoxy resin weight ratio. The image illustrates that the width of the sample remains constant and μ_l values shift in accordance with a change in the concentration. The μ_l readings also increased substantially when different energies were employed with respect to the KCl quantity.

This behavior can be physically interpreted by considering the dominant photon interaction mechanisms. At lower photon energies, the photoelectric effect plays a significant role, leading to higher attenuation coefficients, whereas at higher energies Compton scattering becomes dominant, resulting in a gradual decrease in attenuation values. And this increased reduction can be due to the fact that KCl is better distributed in the epoxy matrix and thus higher density of the material. For this reason, a higher density provides for an easier shielding of gamma rays and increases the linear absorption coefficient [15]. This data also demonstrates that distributing KCl uniformly in epoxy is not only beneficial to the increasing overall efficiency, but it benefits radiation contact as well. As the KCl concentration increases, we see also that uniformity goes up. This renders the material more radiation sensitive and increases both linear attenuation coefficients, μ_l and mass absorption coefficients. A 10% KCl sample exhibited a greater linear attenuation coefficient than

samples of lower concentration, for example. It was attributed to the reason that KCl can be widely dispersed on the surface of material and photons could have higher efficient absorption area. This was a clear indication that efficiency would be enhanced and it would develop well.

Table 2. Measured linear attenuation coefficients of epoxy–KCl composite samples at selected gamma-ray energies.

sample	E(keV)						
	59.4	186	242	295	352	609	662
	^{241}Am			^{246}Ra			^{137}Cs
	μ_l (cm^{-1})						
A	0.137	0.088	0.082	0.078	0.067	0.058	0.057
B	0.159	0.101	0.094	0.090	0.078	0.068	0.066
C	0.179	0.114	0.106	0.101	0.087	0.077	0.074
D	0.196	0.125	0.117	0.110	0.095	0.083	0.081
E	0.215	0.137	0.127	0.122	0.105	0.092	0.089
F	0.236	0.150	0.139	0.134	0.115	0.101	0.098
G	0.257	0.164	0.154	0.145	0.125	0.110	0.106
H	0.273	0.175	0.163	0.154	0.133	0.117	0.113

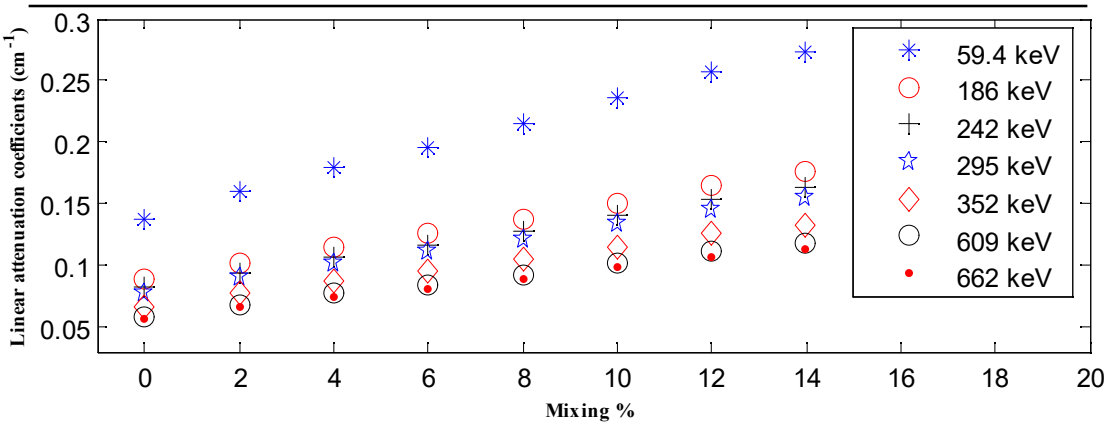

Fig 5. The relationship between the linear attenuation coefficient and mixing percentage.

4.2. The mass attenuation coefficients of potassium chloride (KCl) and epoxy

The mass attenuation coefficient (μ_m) of all the samples was obtained by Eq. (2), and adding the densities from Table 1 under various energy energies and amounts. The summary of these

numbers are presented in Table (3). Figure (6) also represents how the mass attenuation coefficient varies with the mixing ratio and energy of penetrating photon to which it is subjected. The experimental results clearly showed that both mixing ratio and incident photon energy increased the mass attenuation coefficient. Meanwhile, with the increase of the incident photon energy, it caused a decrease in mass attenuation coefficient. This reverse finding arises as a result of the combination between cross-section and incident photon energy in Compton scattering. Essentially, increasing the incident photon energy will reduce the mass attenuation coefficient. All of this is the same as in other studies on photon absorption and it supports what we know about enhanced losses.

Table 3. Measured mass attenuation coefficients of epoxy–KCl composite samples with associated total experimental error at selected gamma-ray energies.

sample	E(keV)						
	59.4	186	242	295	352	609	662
	^{241}Am			^{246}Ra			^{137}Cs
	μ_m(cm^2/g)±Δ μ_m						
A	0.130±0.09	0.083±0.093	0.077±0.097	0.073±0.096	0.063±0.0	0.055±0.095	0.053±0.097
B	0.148±0.08	0.094±0.083	0.087±0.086	0.083±0.082	0.072±0.0	0.063±0.081	0.061±0.086
C	0.164±0.08	0.104±0.081	0.097±0.083	0.092±0.086	0.080±0.0	0.070±0.082	0.068±0.088
D	0.176±0.07	0.112±0.077	0.105±0.079	0.099±0.076	0.085±0.0	0.075±0.077	0.073±0.076
E	0.190±0.07	0.121±0.077	0.112±0.078	0.107±0.076	0.092±0.0	0.081±0.078	0.078±0.077
F	0.2052±0.0	0.130±0.073	0.121±0.073	0.116±0.071	0.100±0.0	0.087±0.073	0.085±0.073
G	0.220±0.08	0.140±0.086	0.131±0.087	0.124±0.084	0.107±0.0	0.094±0.086	0.091±0.087
H	0.230±0.09	0.148±0.93	0.137±0.092	0.130±0.094	0.112±0.0	0.099±0.096	0.095±0.097

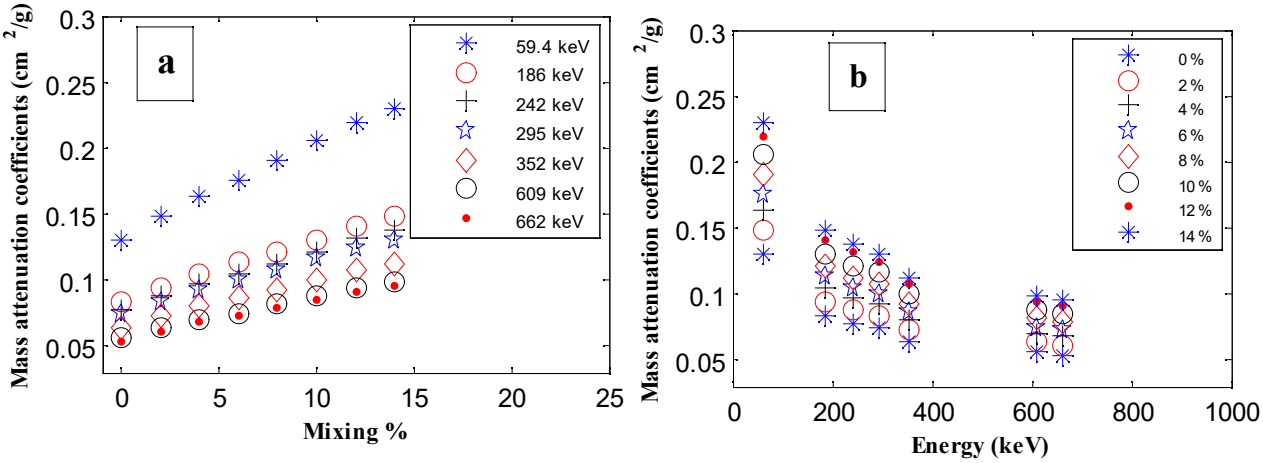

Fig 6. Variation of the mass attenuation coefficient with (a) potassium chloride content and (b) incident gamma-ray energy for epoxy–KCl composites.

The experimentally determined mass attenuation coefficients were evaluated against the reference data provided in the ICRU-44 report. Among all investigated compositions, the composite containing 10 wt.% KCl exhibited the closest agreement with the reference values, with deviations remaining below 7%. Figure 7 presents a direct comparison between the present measurements and the ICRU-44 data, demonstrating the importance of examining the energy-dependent attenuation behavior of candidate tissue-equivalent materials. Such analysis is essential for assessing the extent to which these composites reproduce the radiation interaction characteristics of real biological tissues.

Tissue equivalent materials are of great value to the diagnostic radiologist. The results show that epoxy with potassium chloride (KCl) is a good substitute for tissue-equivalence in nuclear medicine and therapy applications. The selected samples are designed to replicate human tissue properties that are closely related to radiation interactions used in both nuclear medicine and therapy applications.

A comparison with conventional tissue-equivalent materials like polyethylene and paraffin, showed that innovative alternatives achieved better attenuation potential combined to a greater freedom of design - here also without KCl or upon the reduction of KCl. As a result they have wide ranging medical roles; from being used as phantoms for quality control in radiotherapy to contrast agents in diagnostic imaging.

On the financial side of things, these types of revolutionary materials tend to dramatically decrease an initial cost of production, which only means that it shall get cheaper in the long run.

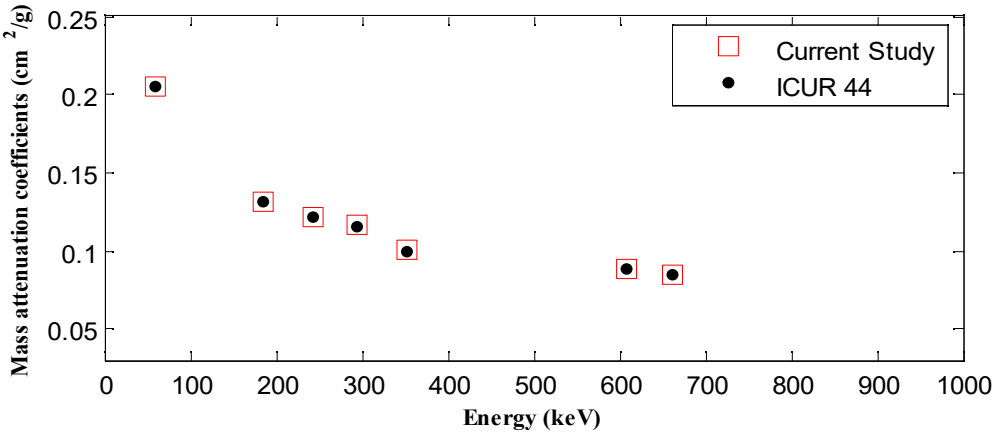

Fig 7. Comparison between the experimentally measured mass attenuation coefficients of sample F and the corresponding reference data from ICRU-44 as a function of photon energy.

4.3. Mean free path attenuation coefficients of potassium chloride (KCl) and epoxy

Means free path (λ) have also been obtained for all as well the Table (1) values with given energies, concentrations and thicknesses from Eq. (3). The experimental data used for these results are presented in Table (4). The table below shows immediately that the mean free path depends on concentration. In particular, these values decrease with increasing concentration of potassium chloride (KCl) at all energy levels. This effect could occur because absorption slows as KCl increases, distributing more of the addition through the base material. This causes the prepared material to be denser in general, and hence more capable of blocking gamma rays. The energy of the inbound photons is also a major contributing factor that modifies mean free path (see Table 4). In Fig. 8 a correlation between the mean open path, mixing ratio and the energy of photons is demonstrated. This scan shows that the mean free path increases with increasing photon energy. This is because various materials interact with gamma rays in different energy ranges. In a higher gas mixing the mean free path will decrease, therefore, as density increases.

Table 4. The experimentally determined mean free path of epoxy resin and potassium chloride (KCl) across various energy levels.

	E(keV)						
	59.4	186	242	295	352	609	662
sample	^{241}Am			^{246}Ra			^{137}Cs
	λ (cm)						
A	7.256	11.334	12.126	12.758	14.906	16.954	17.487
B	6.265	9.854	10.578	11.092	12.812	14.638	15.100

C	5.559	8.709	9.374	9.804	11.396	12.983	13.397
D	5.094	7.937	8.537	9.015	10.447	11.941	12.279
E	4.642	7.286	7.834	8.187	9.518	10.809	11.186
F	4.230	6.630	7.143	7.453	8.670	9.868	10.195
G	3.883	6.079	6.485	6.872	7.957	9.020	9.359
H	3.657	5.683	6.130	6.467	7.499	8.496	8.813

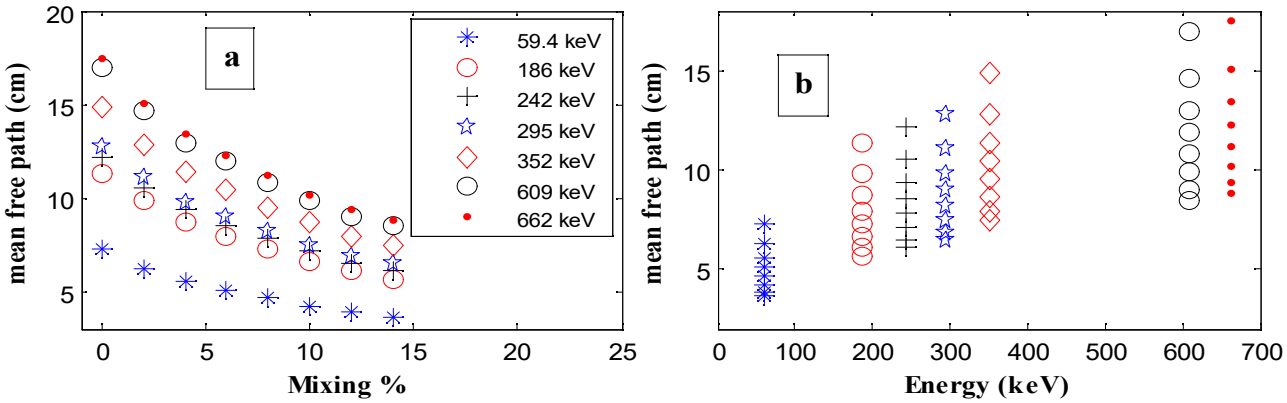

Fig 8. The relationship between the average free path and (a) the proportion of mixing and (b) gamma energy.

5. Conclusion

After the research, a mixture containing 90% epoxy resin and 10% potassium chloride (KCl) was found optimal for making a human tissue equivalent. The tested energy values of all the samples in this study were effectively assessed within the range of 662 to 59.4 keV. The experimental mass attenuation coefficients are relatively well correlated to those obtained from the data from the ICRU-44 report. This consistency only gives more validity to the data and supports the promising use of these materials in medicine as well as radiation for medical and radiotherapy. For example, they could be used to develop quality assurance models for radiotherapy, since they model human tissue. Additionally, due to their consistency with ICRU-44 data, they also enhance the applicability to radiation dosimetry, and that can enhance the accuracy of dose measurement and reduce errors in the radiotherapy procedure during dosage titration. Consequently, these materials are seen as good candidates for a range of medical applications, including imaging for diagnosis and radiotherapy. It is thus advisable to use sample F of the tissue equivalent materials to model how radiation acts on the human body in nuclear medicine and in therapeutic fields.

Declarations

Availability of data and material: This article has no associated data.

Author contributions: The present experimental study was performed by Lina Asker Muhammad Ali in partial fulfillment of the requirements for the Ph.D. degree. She conducted the experimental work, measurements, data analysis, and initial drafting of the manuscript. The research was carried out under the supervision of Rasha Hamid Ahmed and Mohsin Hassan Ali, who provided continuous academic supervision, methodological guidance, and critical revision of the manuscript.

Acknowledgements: The authors would like to thank the administration of Tikrit University for their support and encouragement during this work.

Funding: The authors declare no funding of this study.

Conflict of interest: The authors declare that there is no conflict of interest regarding the publication of this work.

References

1. Jones, A.K.; Hintenlang, D.E.; Bolch, W.E. Tissue-equivalent materials for construction of tomographic dosimetry phantoms in pediatric radiology. *Medical Physics* 2003, 30(8), 2072–2081. https://doi.org/10.1118/1.1592641
2. White, D.R.; Booz, J.; Griffith, R.V.; Spokas, J.J.; Wilson, I.J. *Tissue Substitutes in Radiation Dosimetry and Measurement*, ICRU Report 44; International Commission on Radiation Units and Measurements: Bethesda, MD, USA, 1989.
3. Amini, I.; Akhlaghi, P.; Sarbakhsh, P. Construction and verification of a physical chest phantom from suitable tissue-equivalent materials for computed tomography examinations. *Radiation Physics and Chemistry* 2018, 150, 51–57. https://doi.org/10.1016/j.radphyschem.2018.04.020
4. Apaza, G.; Chen, F.; Vega, J. Construction and characterization of materials equivalent to the tissues and organs of the human body for radiotherapy. *Radiation Physics and Chemistry* 2019, 159, 70–75. https://doi.org/10.1016/j.radphyschem.2019.01.013
5. Hasanzadeh, H.; Abedelahi, A. Introducing a simple tissue-equivalent anthropomorphic phantom for radiation dosimetry in diagnostic radiology and radiotherapy. *Iranian Journal of Medical Physics* 2011, 2(4), 25–29.
6. Followill, D. S. Anthropomorphic phantoms for radiation oncology medical physics. In *The Phantoms of Medical and Health Physics*; Springer: Berlin, Germany, 2013; pp. 39–51. https://doi.org/10.1007/978-1-4614-8304-5_3
7. El Bardouni, T.; El Hajjaji, O.; Al-Kanti, H.; Arectout, A.; El-Mugahed, A.; et al. Validation and investigation of mass attenuation coefficients calculations in different parts of adult human body organ using GAMOS code. *Radiation Physics and Chemistry* 2025, 239, 113271. https://doi.org/10.1016/j.radphyschem.2025.113271
8. Mohammed, S.I.; Taqi, A.H. Mass attenuation coefficient of electromagnetic radiation for human tissues. *Journal of Radiation Research and Applied Sciences* 2025, 18, 101255. https://doi.org/10.1016/j.jrras.2024.101255
9. Rafiei, M.; Parsaei, S.; Kaur, P.; Singh, K.J.; Büyükyıldız, M. A Monte Carlo investigation of some important radiation parameters and tissue equivalency for photons below 1 keV in human tissues. *Biomedical Physics & Engineering Express* 2022, 8(2), 025002. https://doi.org/10.1088/2057-1976/ac428f
10. Haider, R.D.; Ismail, A.H.; Hussein, Z.A. Study of heavy and trace metal concentrations in rabbit teeth for species identification using X-ray fluorescence and mass attenuation coefficients. *Applied Radiation and Isotopes* 2025, 228, 112321. https://doi.org/10.1016/j.apradiso.2025.112321
11. Molina Higgins, M.C.; Radcliffe, N.A.; Toro-González, M.; Rojas, J.V. Gamma-ray attenuation of hafnium dioxide- and tungsten trioxide-epoxy resin composites. *Journal of Radioanalytical and Nuclear Chemistry* 2019, 322(2), 613–622. https://doi.org/10.1007/s10967-019-06714-3
12. Ragheb, M. *Radiation Physics*, 3rd ed.; John Wiley and Sons: New York, NY, USA, 2007.
13. National Institute of Standards and Technology (NIST). X-ray mass attenuation coefficients; NIST: Gaithersburg, MD, USA, 2013.

14. Hubbell, J.H.; Seltzer, S.M. Tables of X-Ray of Mass attenuation coefficient and mass energy absorption coefficient 1 KeV to 20 MeV for elements Z=1 to 92 and 48 additional substances of dosimetric interest. NISTIR 5632; National Institute of Standards and Technology: Gaithersburg, MD, USA, 1995.
15. Awasarmol, V.V.; Gaikwad, D.K.; Raut, S.D.; Pawar, P.P. Photon interaction study of organic nonlinear optical materials in the energy range 122 – 1330 keV. *Radiation Physics and Chemistry* 2017, 130, 343–350. https://doi.org/10.1016/j.radphyschem.2016.09.012
16. Aytaç Levet; Kaur, P.; Kahruman, C.; Thakur, S.; Büyükyıldız, M. Brass alloys improved with antimony additives for gamma-ray shielding applications. *Applied Radiation and Isotopes* 2026, 288, 112313. https://doi.org/10.1016/j.radphyschem.2016.09.012
17. Sayyed, M.I. Half value layer, mean free path and exposure buildup factor for tellurite glasses with different oxide compositions. *Journal of Alloys and Compounds* 2017, 695, 3191–3197. https://doi.org/10.1016/j.jallcom.2016.11.318